



## Mesoporous carbide-derived carbon for cytokine removal from blood plasma

Saujanya Yachamaneni<sup>a</sup>, Gleb Yushin<sup>b</sup>, Sun-Hwa Yeon<sup>a</sup>, Yury Gogotsi<sup>a,\*</sup>, Carol Howell<sup>c</sup>, Susan Sandeman<sup>c</sup>, Gary Phillips<sup>c</sup>, Sergey Mikhalovsky<sup>c</sup>

<sup>a</sup> Department of Materials Science and Engineering and A.J. Drexel Nanotechnology Institute, Drexel University, Philadelphia, PA 19104, USA

<sup>b</sup> School of Materials Science and Engineering, Georgia Institute of Technology, Atlanta, GA 30332-0245, USA

<sup>c</sup> The Centre for Biomedical and Health Science Research, University of Brighton, Brighton BN2 4GJ, UK

### ARTICLE INFO

#### Article history:

Received 18 January 2010

Accepted 21 February 2010

Available online 19 March 2010

#### Keywords:

Carbide derived-carbon

Protein adsorption

Cytokine

MAX phase

Mesoporous carbon

Sepsis

### ABSTRACT

Porous carbons can be used for purification of bio-fluids due to their excellent biocompatibility with blood. Since the ability to adsorb a range of inflammatory cytokines within the shortest possible time is crucial to stop the progression of sepsis, the improvement of the adsorption rate is a key factor to achieving efficient removal of cytokines. Here, we demonstrate the effect of synthesis temperatures (from 600 °C to 1200 °C), carbon particle sizes (from below 35 μm to 300 μm), and annealing conditions (Ar, NH<sub>3</sub>, H<sub>2</sub>, Cl<sub>2</sub>, and vacuum annealing) that determine the surface chemistry, on the ability of carbide-derived carbons (CDCs) to remove cytokines TNF-α, IL-6, and IL-1β from blood plasma. Optimization of CDC processing and structure leads to up to two orders of magnitude increase in the adsorption rate. Mesoporous CDCs that were produced at 800 °C from Ti<sub>2</sub>AlC with the precursor particle size of <35 μm and annealed in NH<sub>3</sub>, displayed complete removal of large molecules of TNF-α in less than an hour, with >85% and >95% TNF-α removal in 5 and 30 min, respectively. This is a very significant improvement compared to the previously published results for CDC (90% TNF-α removal after 1 h) and activated carbons. Smaller interleukin IL-6 and IL-1β molecules can be completely removed within 5 min. These differences in adsorption rates show that carbons with controlled porosity can also be used for separation of protein molecules.

© 2010 Elsevier Ltd. All rights reserved.

### 1. Introduction

Sepsis syndrome, which is a major threat to the contemporary population with the overall mortality rate of 40–80%, represents a systemic response to infection. It results from an excessive host inflammatory response to a specific inciting event such as a micro-biologically confirmed infection of gram-negative or positive bacteria that leads to tissue injury [1,2]. Sepsis induced by the release of invading pathogenic microorganism components into the host, is characterized by the release of excessive amounts of pro and anti-inflammatory cytokines, such as tumor necrosis factor-α (TNF-α), interleukin-1β (IL-1β), IL-8, and IL-6, into the circulation [3].

Continuous renal replacement therapies (CRRTs) may reduce this excessive inflammatory response by nonspecific extracorporeal removal of cytokines and has been shown to improve cardiovascular hemodynamics [3]. Although CRRT extracorporeal removal of inflammatory mediators has been confirmed in clinical studies, few have reported significant effects on cytokine plasma concentrations and little was shown with regard to the concomitant removal of

inhibitors of inflammation [4–6]. Alternative methods of selected inflammatory cytokine removal, such as continuous hemofiltration and hemodiafiltration, have been studied [3,7]. In previous studies *in vitro* continuous plasma filtration coupled with adsorption by charcoal, different resins, and carbonized powders, achieved removal efficiency of IL-1β, IL-6, and IL-8 in the range of 94–100%. However, the concentration of TNF-α, which has larger molecular dimensions than others, could only be decreased by 20–80% depending on the adsorbent [7,8]. Even the best mesoporous carbons [9,10], surface saturation occurred quickly, limiting the sorption of TNF-α. Better results were achieved using sophisticated cellulose microparticles functionalized either with a monoclonal anti-TNF antibody or with recombinant human antibody fragments, but still complete removal of TNF-α was not achieved after an hour-long exposure [11]. Since time of extracorporeal treatment is limited to several hours within which to halt the progression of sepsis and to save a patient's life, it is critical to choose or design new adsorbents with improved TNF-α adsorption efficiency and kinetics for this important cytokine.

Activated carbons (ACs) are the most powerful conventional adsorbents, mainly due to their highly developed porous structures and very large surface areas (above 1000 m<sup>2</sup>/g). Many specially purified activated carbons prepared from synthetic polymers also

\* Corresponding author. Tel.: +1 215 895 6446; fax: +1 215 895 1934.

E-mail address: [gogotsi@drexel.edu](mailto:gogotsi@drexel.edu) (Y. Gogotsi).

show excellent biocompatibility, such as (i) moderate levels of monocyte and granulocyte adhesion in conjunction with adsorption of plasma proteins to the carbon surface, and (ii) no activation of granulocyte and adherent platelets as well as no activated complement cascade by the carbons. They do not require a special coating for direct contact with blood suggesting the carbon surface has a passivating effect [12]. Also, the study of the cytokine removal from plasma by the activated carbon device in a flowing system has proven that the system did not exacerbate the pro-coagulant state by excessive removal of plasma proteins or clotting factors or by direct activation of the intrinsic coagulation pathway [9,10]. However, the majority of pores in ACs are generally <2 nm, which limits their performance in adsorption of large biomolecules, such as TNF- $\alpha$ . For mesoporous carbon, a templating procedure using sacrificial inorganic templates has been proposed for the formation of larger pores and achieving a more uniform pore size distribution that leads to improved adsorption capacity [13,14].

Carbide-derived carbons (CDCs) produced by etching of metal from metal carbides have recently been shown to offer great potential for controlling the size of both micropores (0.4–2 nm) [15,16] and mesopores (2–50 nm) [17,18]. The study of adsorption of cytokines using slit-shaped mesoporous CDCs synthesized from selected ternary (MAX-phase) carbides has demonstrated high cytokine removal efficiency in certain CDC samples, which resulted from their tunable pore size and large pore volume [19]. While the CDC adsorbents, especially derived from Ti<sub>2</sub>AlC, outperformed other materials or methods for the efficient removal of TNF- $\alpha$ , the maximum removal efficiency of TNF- $\alpha$  was less than 90% and was achieved on the CDC prepared from Ti<sub>2</sub>AlC at 800 °C. Several strategies can be explored in order to further improve protein adsorption efficiency. First, annealing of CDCs synthesized by chlorination of carbides will contribute to pore opening and increase the available volume of open pores, thus providing more surface area available for adsorption. Second, the particle size can be reduced in order to improve the sorption kinetics. Metal carbide powders are available with particle sizes ranging from nanometers to hundreds of micrometers. Because the carbide-to-CDC transformation is conformal, it is possible to manipulate the particle size of CDC by changing the particle size of initial metal carbide precursor.

Here we report a study of the effect of synthesis temperatures (from 600 °C to 1200 °C), carbide particle sizes (from below 35  $\mu$ m to 300  $\mu$ m), and annealing conditions (Ar, NH<sub>3</sub>, H<sub>2</sub>, Cl<sub>2</sub>, and vacuum annealing) on the structure and porosity of CDCs synthesized from Ti<sub>2</sub>AlC carbide, and investigated the effect of pore structure on the removal of cytokines (TNF- $\alpha$  and IL-6) from blood plasma.

## 2. Materials and methods

### 2.1. Materials

CDCs were synthesized from Ti<sub>2</sub>AlC powders by the reaction with pure chlorine (99.5%, BOC gases) at 600–1000 °C. The carbide was produced at Drexel University, but is now commercially available (3-ONE-2, Inc, NJ, US). Ti<sub>2</sub>AlC belongs to the MAX-phase group of ternary carbides, having a layered hexagonal structure with carbon atoms positioned in basal planes and separated by 0.68 nm (Ti<sub>2</sub>AlC). The CDCs produced from MAX-phase carbides are known to possess slit-shaped open pores [16,17,20].

Ti<sub>2</sub>AlC was drilled by a drill machine using drill bits made of high-speed steel. The powder produced was coarse and had a very wide distribution of particle sizes ranging from few micrometers to millimeters in size. To obtain more narrow particle size distribution, this powder was crushed further using a zirconia mortar. The powder obtained from drilling and from grinding in a mortar was then separated into 4 different fractions, 0–38  $\mu$ m, 38–45  $\mu$ m, 106–150  $\mu$ m, and 106–300  $\mu$ m. The obtained powder was then characterized by microscopy to determine the efficiency of the particle separation and determine the exact composition and purity of the carbide. After screening of the powder to different sizes, Scanning Electron Microscopy (SEM) micrographs were recorded (Philips XL-30) in order to verify the separation efficiency. For CDC synthesis, the selected carbide powder was placed onto a quartz sample holder and loaded into the hot zone of a horizontal quartz tube

furnace. Prior to heating, the tube (~30 mm in diameter) was purged with high purity Ar (BOC Gases, 99.998%) for 30 min at a flow rate of 100 sccm. Once the desired temperature was reached and stabilized, the Ar flow was stopped and a 3-h chlorination began with Cl<sub>2</sub> flowing at a rate of 10 sccm. After the completion of the chlorination process, the samples were annealed under a flow of Ar, Cl<sub>2</sub>, H<sub>2</sub> or NH<sub>3</sub> (40 sccm) at 800 °C for about 5 h to remove any residual chlorine or metal chlorides from the pores, and taken out for further analyses. For vacuum annealing, the samples were heated at 1300 °C for 5 h *in vacuo*. A detailed description of the chlorination apparatus used in this study can be found elsewhere [19–21].

### 2.2. Characterization

The porosity of the CDC was measured by analyzing argon sorption isotherms recorded at 77 K using Quadrasorb (Quantachrome Instruments, USA). The pore size analysis software, Quadrawin version 1.1, was used for the analysis. The Ar sorption isotherms were obtained at liquid nitrogen temperature (~196 °C) in the relative pressure P/P<sub>0</sub> range of about 2  $\times$  10<sup>-2</sup>–1. The isotherms were analyzed using Brunauer–Emmett–Teller (BET) equation and non-local density functional theory (NLDFT) to determine the specific surface area (SSA) and pore-size distribution (PSD) of the CDCs. The SSAs calculated using BET or DFT theory are referred to as BET-SSA or DFT-SSA, respectively. A difference in absolute values between BET-SSA and DFT-SSA is expected, as both types of calculations are based on different assumptions, which might not be justified with the utmost accuracy for all the materials under study. Quantachrome Instruments data reduction software Autosorb v.1.50 was employed for the porosity analysis. Slit-shaped pores were assumed for the calculations.

To determine the chemical composition of the CDC, SEM analysis was carried out in conjunction with energy dispersive spectroscopy (EDS). Zeiss Supra 50VP Scanning Electron Microscope was used for taking high-resolution SEM images of the CDC samples. Renishaw 1000 micro-Raman spectrometer with an Ar ion laser (514.5 mm) collect Raman spectra (spot size ~ 2  $\mu$ m). D- and G- bands of sp<sup>2</sup> carbon, located at about 1360 and 1590 cm<sup>-1</sup>, respectively, were fit with Gaussian and Lorentzian peaks, GRAMS/32 software from Renishaw, UK was used for data analysis.

### 2.3. Cytokine adsorption experiments

Fresh frozen human plasma (NBS, UK) was defrosted and spiked with the recombinant human cytokines (TNF- $\alpha$ , IL-6, and IL-1 $\beta$  all obtained from BD Biosciences, USA) at a concentration of 1000 pg/ml. These levels are comparable with the concentrations measured in the plasma of patients with sepsis [2,4,22]. Carbon adsorbents (0.02 g) were equilibrated in phosphate-buffered saline (PBS) (0.5 ml) overnight prior to removal of PBS and addition of 800  $\mu$ l of spiked human plasma. Controls consisted of spiked and unspiked plasma with no adsorbent present. Adsorbents were incubated at 37 °C while shaking (90 rpm). At 5, 30 and 60 min time points, samples were centrifuged (125 g) and the supernatant collected and stored at -20 °C prior to ELISA (BD Biosciences) analysis for the presence of cytokines. Samples were diluted 1:4 (TNF- $\alpha$ ) and 1:10 (IL-6 and IL-1 $\beta$ ) in assay diluents prior to analysis. In order to obtain the percentage of cytokines (TNF- $\alpha$ , IL-6, and IL-1 $\beta$ ) removed from spiked plasma the cytokine amount of control was used as the initial amount.

## 3. Results and discussion

EDS analysis revealed that the powders of Ti<sub>2</sub>AlC with the broad particle size distribution, 0.5–500  $\mu$ m, were fully chlorinated for all temperatures and complete removal of metal atoms was ensured with complete conversion of the carbide into carbon in the particle size range [18].

Fig. 1(a–e) shows typical SEM micrographs of Ti<sub>2</sub>AlC particles and mesoporous Ti<sub>2</sub>AlC–CDC synthesized at 800 °C. The as-received Ti<sub>2</sub>AlC carbide (inset in Fig. 1a and b) with flake-like grains shows a lamellar structure of a typical MAX phase which has a preferred orientation with the basal planes [23–25]. The mesoporous CDCs also show a layered carbon structure (Fig. 1(c–e)). The edges of carbon lamella were covered with mesoporous carbon spherulites of the size ~ 0.3  $\mu$ m (Fig. 1e). EDS confirmed the removal of Ti and Al to the level below 1 wt% (Table 1). Raman spectroscopy analysis of Ti<sub>2</sub>AlC–CDCs synthesized at 600–1000 °C (Fig. 3f) exhibits typical D (~1340 cm<sup>-1</sup>, breathing mode) and G (1591 cm<sup>-1</sup>, in-plane vibrational mode) bands of disordered carbon. However, the G band in the 1000 °C sample is split by a broad shoulder and exhibits the shift from about 1591 cm<sup>-1</sup> to 1585 cm<sup>-1</sup>, approaching graphite at 1582 cm<sup>-1</sup> [26]. In this spectrum, a broad shoulder at 1620 cm<sup>-1</sup>, close to the G band, is attributed to the D' band which corresponds to

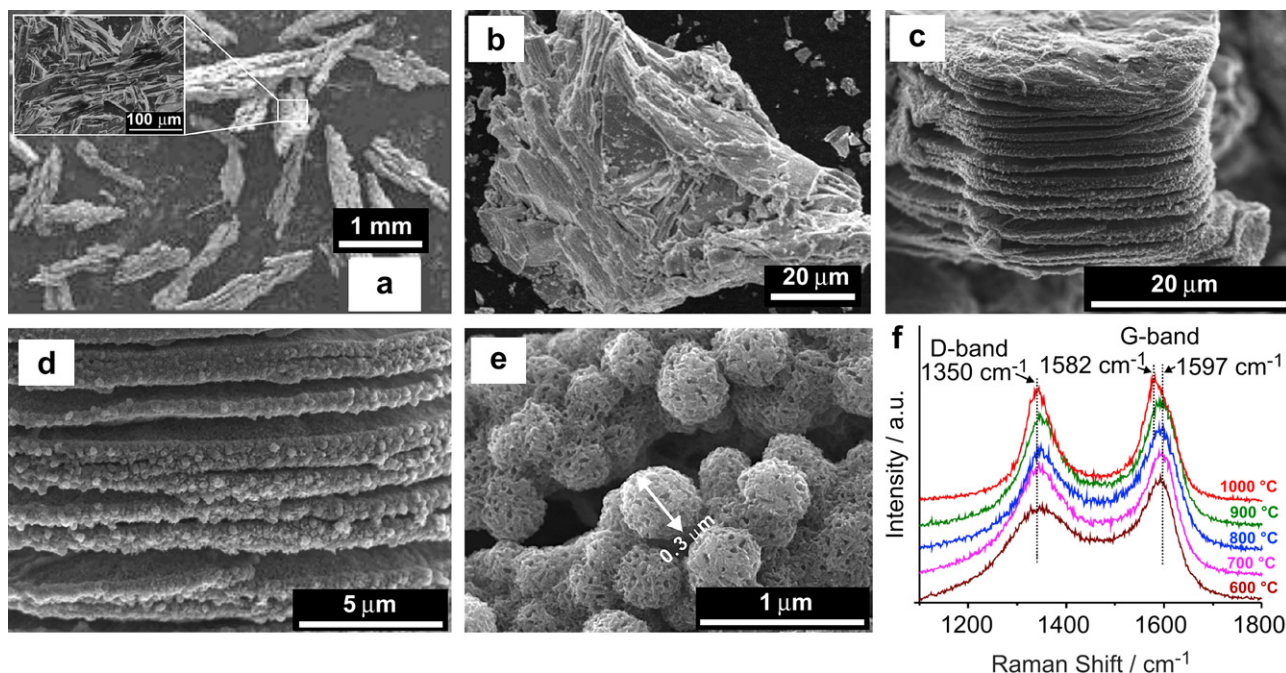


**Fig. 1.** SEM images of  $\text{Ti}_2\text{AlC}$  with various particle sizes (106–300  $\mu\text{m}$  (a), 38–45  $\mu\text{m}$  (b)) and  $\text{Ti}_2\text{AlC-CDC}$  chlorinated at 800  $^\circ\text{C}$  (c–e). Raman spectra (f) of  $\text{Ti}_2\text{AlC-CDCs}$  chlorinated at the indicated temperatures.

the highest wavenumber feature in the density of states indicating a forbidden structure under defect-free conditions [27]. D band becomes more narrow as the synthesis temperature increases, indicating the increase in carbon crystallinity.

Figs. 2 and 3 compare efficiency of removal of two selected cytokines (tumor necrosis factor alpha (TNF- $\alpha$ ) and interleukin-6 (IL-6)) from human plasma using the mesoporous CDCs, which were synthesized from  $\text{Ti}_2\text{AlC}$ , as a function of particle size, synthesis temperature, and annealing conditions. Another cytokine, IL-1 $\beta$ , was completely removed from blood plasma within 5 min by all samples under study and no data plotting was necessary. TNF- $\alpha$  has a molecular weight ranging from 17 to 51 kDa depending on whether it is found in the monomer, dimer, or trimer state [28]. Among them, a homotrimer is the most active form of TNF- $\alpha$ , which has the largest dimension of all cytokines with the crystal structure of space group  $P4_12_12$  ( $a = 9.4$  nm  $b = 9.4$  nm  $c = 11.7$  nm) [28,29]. Due to the large size of the trimeric form of this cytokine, adsorption of TNF- $\alpha$  is a challenging task [8, 19].

Adsorption of TNF- $\alpha$  was successfully increased by decreasing the precursor particle size, as shown in Fig. 2a for CDC synthesized at 800  $^\circ\text{C}$ . The smallest CDC particles with dimensions  $< 38$   $\mu\text{m}$

removed 99.7% of the TNF- $\alpha$  within 60 min (Fig. 2a). Interestingly, all the CDC particles showed similar levels of TNF- $\alpha$  adsorption with 5 and even 30 min incubation, when the adsorption is presumably limited to the outer surface layer of carbon particles. However, the TNF- $\alpha$  adsorption rate for larger particles slows down significantly during the longer adsorption time. The observed phenomenon could be related to slow diffusion of large TNF- $\alpha$  molecule within CDC pores and to partial blocking of the pores by the cytokines adsorbed within the first 30 min. When compared to our prior studies, where CDC with no intensive purification adsorbed less than 92% of TNF- $\alpha$  within 60 min [19], the latest CDC samples of virtually any size in the range from below 38 to above 300  $\mu\text{m}$ , showed excellent adsorption characteristics and 95–99.7% removal efficiency. The more elaborate and efficient purification of CDC from the remaining chlorides and chlorine in the present work (samples were purged in the stream of Ar for about 5 h at 800  $^\circ\text{C}$  in the present studies, as compared 15 min purge in Ar in the prior work) is a likely cause of more efficient adsorption. The blocking of pores by the remaining chlorides may slow down diffusion of large cytokines into the core of the CDC particles. It is also possible that chlorine or chlorides cause a stronger adhesion of cytokines to the CDC surface,

**Table 1**  
Characterization results of porous  $\text{Ti}_2\text{AlC-CDCs}$ .

Particle size ( $\mu\text{m}$ )	$\text{Cl}_2$ Temp. ( $^\circ\text{C}$ )	Annealing 800 $^\circ\text{C}$	BET SSA ( $\text{m}^2/\text{g}$ )	DFT SSA ( $\text{m}^2/\text{g}$ ) <sup>a</sup>	SSA Pore $< 5$ nm <sup>a</sup>	SSA Pore $< 9.5$ nm <sup>a</sup>	SSA Pore $> 9.5$ nm <sup>a</sup>
38–45	800	Ar	1490	1140	999	1079	61
106–300	800	Ar	1552	1201	989	1098	103
106–150	800	$\text{H}_2$	1490	1140	999	1079	61
106–150	800	$\text{NH}_3$	1552	1201	989	1098	103
106–150	800	$\text{Cl}_2$	1208	950	845	913	37
106–150	800	Ar	1199	904	776	812	92
$< 38$	600	$\text{H}_2$	1850	1414	1228	1350	64
$< 38$	700	$\text{H}_2$	1750	1316	1147	1256	60
$< 38$	800	$\text{H}_2$	1150	904	714	824	80
$< 38$	900	$\text{H}_2$	1080	856	671	782	74
$< 38$	1000	$\text{H}_2$	1580	1259	1101	1201	49

<sup>a</sup> DFT Specific Surface Area (SSA) and SSA of pores of different width were calculated for slit pores using the Nonlocal Density Functional Theory (NLDFT) method from Ar sorption isotherms obtained at 77 K. All samples were outgassed at 200  $^\circ\text{C}$  for 24 h before Ar sorption.

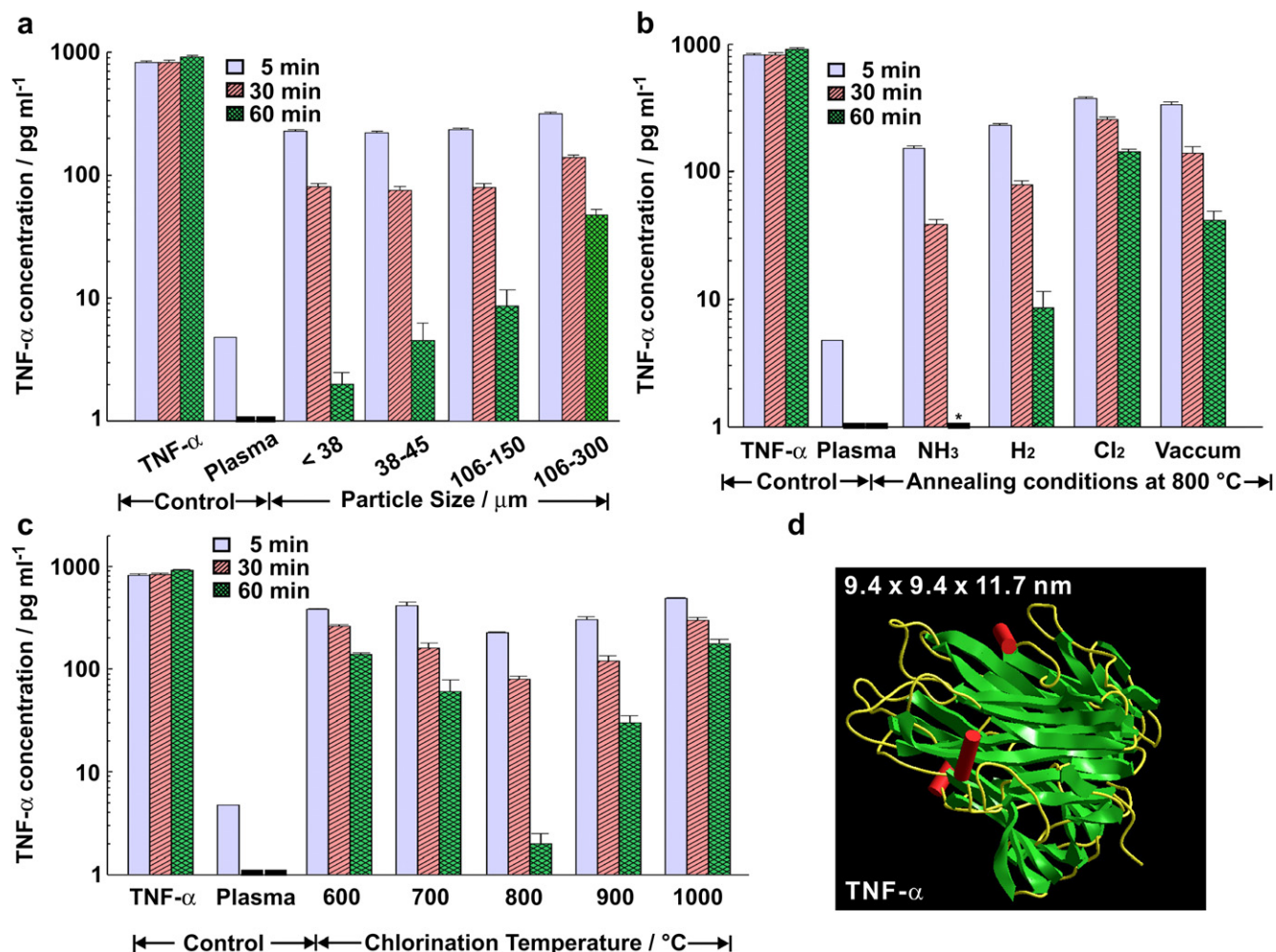


**Fig. 2.** Logarithmic plots of carbide-derived carbon adsorption of TNF- $\alpha$  from human plasma. Plasma spiked with cytokines was collected after contact with CDCs as a function of (a) precursor particle sizes (all CDCs were chlorinated at 800 °C for 3 hr and annealed in Ar), (b) annealing conditions (all CDCs were chlorinated at 800 °C for 3 h using the precursor of 38–45  $\mu$ m), and (c) chlorination temperature (all CDCs were annealed in H<sub>2</sub> at 800 °C for 2 h after chlorination using the precursor of <38  $\mu$ m), and assayed for cytokine concentration by ELISA ( $n = 4$ , mean  $\pm$  SEM). Asterisk shows 100% removal of cytokine from the plasma. (d) HyperChem model of the structure and dimension of TNF- $\alpha$  based on crystallographic data from Ref. [31].

creating the “traffic jams” on the particle surface and preventing cytokine diffusion into the bulk of the particles. The purification process performed by CDC annealing under continuous Ar purge has its limitations and is incapable of removing chlorine and open the blocked pores completely (Table 2). In an attempt to further improve the purification efficiency and remove residual non-carbon species within the carbon pore network, the CDCs were annealed in NH<sub>3</sub>, H<sub>2</sub>, Cl<sub>2</sub>, and vacuum and their removal efficiencies for TNF- $\alpha$  and IL-6 were investigated. The CDC annealed in NH<sub>3</sub> after chlorination at 800 °C demonstrated 100% adsorption after 60 min, which is remarkable for TNF- $\alpha$  adsorption compared to Adsorba 300C (Norit) carbon, which is used for hemoperfusion, the mesoporous Acti-carbone CXV (Ceca, France), and previously reported CDCs [19]. Even in the case of expensive sorbents with attached monoclonal anti-TNF antibodies or recombinant human antibody fragments, the maximum removal of TNF- $\alpha$  only reached  $\sim$ 95% after 60 min [11]. As the relationship between protein removal efficiency and porous structure of carbon has been interpreted by previous studies [8,19], this outstanding adsorption result is likely due to an increase in SSA of pores larger than 9.5 nm, which are accessible to TNF- $\alpha$ , by opening the blocked pores, reduced surface of carbon resulting from the ammonia treatment and complete removal of chlorine and

chloride molecules from the pores. The efficiency of TNF- $\alpha$  removal in CDC annealed in vacuum and chlorine is 96% and 75%, respectively. The Cl<sub>2</sub> treated CDC shows the smallest SSA of accessible pores and the lowest cytokine removal efficiency. Nevertheless, the high total BET SSA (1208 m<sup>2</sup>/g) of the Cl<sub>2</sub> treated CDC is quite high and comparable with that of Ar annealed CDCs (Table 1). This discrepancy between low removal efficiency and high BET SSA may be caused by outgassing process always performed prior to sorption analysis which can remove Cl<sub>2</sub> molecules.

In the study of the effect of CDC synthesis temperature in the range from 600 to 1000 °C, the 800 °C sample showed the highest SSA of pores >9.5 nm and the highest TNF- $\alpha$  removal efficiency, 99.8% within 60 min. The samples produced at 1000 °C showed a lower removal efficiency of 75%. This result is supported by mesoporous isotherm trends revealed by Ar and N<sub>2</sub> sorption at 77 K [18]. CDCs prepared from ternary carbides such as Ti<sub>2</sub>AlC or Ti<sub>3</sub>AlC<sub>2</sub> showed large hysteresis loops indicating a large volume of mesopores (1.6 cm<sup>3</sup>/g for mesopores (>2 nm) + 0.4 cm<sup>3</sup>/g for micropores (<2 nm)) only at 800 °C. However, at 1000 °C, the mesopore volume decreased to 1.3 cm<sup>3</sup>/g and the micropore volume increased to 0.6 cm<sup>3</sup>/g, respectively [18]. These trends are not in accord with the CDCs derived from binary carbides (TiC, SiC, or ZrC)

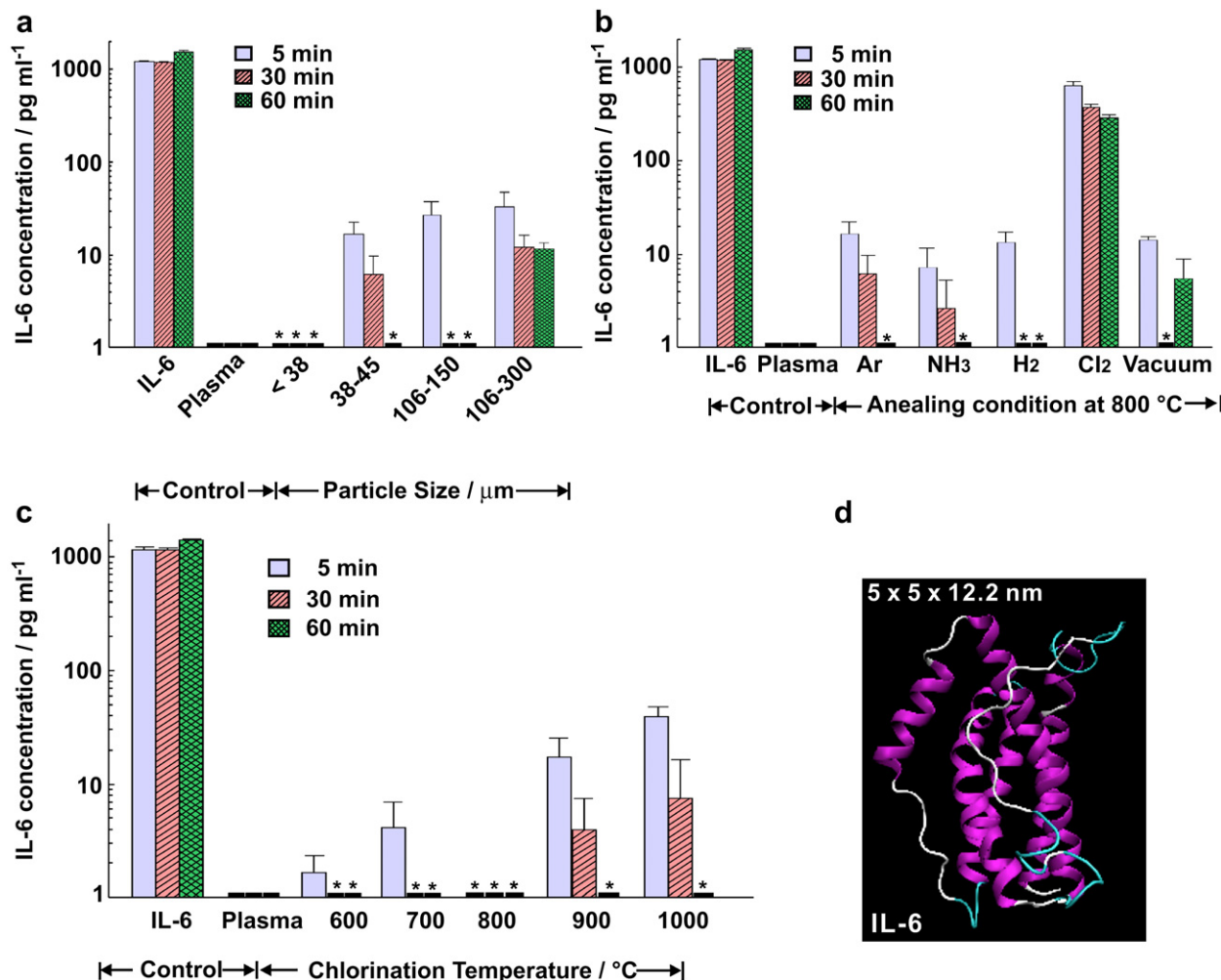


**Fig. 3.** Logarithmic plots of carbide-derived carbon adsorption of the cytokines (IL-6) from human plasma. Plasma spiked with cytokines was collected after contact with CDCs as a function of (a) precursor particle sizes (all CDCs were chlorinated at 800 °C for 3 hr and annealed in Ar), (b) annealing conditions (all CDCs were chlorinated at 800 °C for 3 hr using the precursor of 38–45  $\mu\text{m}$ ), and (c) chlorination temperature (all CDCs were annealed in H<sub>2</sub> at 800 °C for 2 h after chlorination using the precursor of <38  $\mu\text{m}$ ), and assayed for cytokine concentration by ELISA ( $n = 4$ , mean  $\pm$  SEM). Asterisk shows 100% removal of cytokine from the plasma. (d) HyperChem model of the structure and dimension of IL-6 based on crystallographic data from Ref. [32].

which demonstrate the tendency of increasing mesopore volume with increases of synthesis temperature, due to loss of carbon atoms and the collapse of the carbon structure [21].

Fig. 3 shows the adsorption of the interleukin-6 (IL-6) with the crystal structure of  $a = 5$  nm,  $b = 5$  nm, and  $c = 12.2$  nm, which is composed of the four main helices and their long loop [30]. IL-6 with the relatively narrow and long dimension was adsorbed into the CDC very rapidly and efficiently, as compared to TNF- $\alpha$ . In all the particle size ranges, the cytokine removal efficiency was in excess of 99% after 60 min (Fig. 3a). Depending on the annealing conditions and synthesis temperature, the removal tendencies are consistent with TNF- $\alpha$ , but the kinetics of the process was faster, with 97% or more of IL-6 adsorbed within the first 5 min.

**Table 2**  
Elemental composition (at %) of porous Ti<sub>2</sub>AlC-CDCs chlorinated at 800 °C (based on EDS data).

Annealing at 800 °C in:	Ar	H <sub>2</sub>	NH <sub>3</sub>
C	85	86	80
Cl	5.8	1.51	0.21
Al	1.14	0.13	0.54
Ti	0.05	0.08	0

#### 4. Conclusions

The removal efficiency of cytokines (TNF- $\alpha$ , IL-6, and IL-1 $\beta$ ) was studied on mesoporous graphitic CDCs synthesized by chlorination of layered ternary MAX phase carbide Ti<sub>2</sub>AlC. The CDC particle size, surface chemistry, and synthesis temperature were varied. The results showed very high removal efficiency of TNF- $\alpha$  of up to  $\sim$  99.7% by 60 min in the case of CDC post-annealed in Ar at 800 °C for 5 h and synthesized from the precursor particles of <38  $\mu\text{m}$ . This efficiency was further improved to 100% when the annealing environment was changed from Ar to NH<sub>3</sub>. The adsorption rate of IL-6 with relatively small dimensions was much faster in the first 5 min than that for TNF- $\alpha$ . Its removal reached 100% after 60 min for all but CDC annealed in Cl<sub>2</sub>. The adsorption rate of the smallest IL-1 $\beta$  cytokine was the fastest, with 100% removal reached in 5 min for all the samples (data not shown). From the pore texture analysis, it was confirmed that the removal of cytokines is affected by the relationship between adsorbate critical molecular size and CDC pore size which can be optimized by tuning the synthesis temperature, and post-synthesis annealing. The particle size and surface chemistry also play an important role and can be optimized for the selective sorption of various biomolecules. The synthesized

mesoporous CDCs are very effective for protein adsorption from blood plasma.

## Acknowledgements

This work was supported by the US National Science Foundation, grant DMR-0945230. We acknowledge use of instruments (Raman spectrometer and SEM) in the Centralized Research Facility of Drexel University and Prof. M Barsoum (Drexel University) for providing a Ti<sub>2</sub>AlC sample.

## Appendix

Figures with essential colour discrimination. Most of the figures in this article have parts that are difficult to interpret in black and white. The full colour images can be found in the on-line version, at doi:10.1016/j.biomaterials.2010.02.054.

## References

- [1] Blackwell TS, Christman JW. Sepsis and cytokines: current status. *Br J Anaesth* 1996;77(1):110–7.
- [2] Cohen J, Abraham E. Microbiologic findings and correlations with serum tumor necrosis factor- $\alpha$  in patients with severe sepsis and septic shock. *J Infect Dis* 1999;180(1):116–21.
- [3] De Vriese AS, Colardyn FA, Philippe JJ, Vanholder RC, De Sutter JH, Lameire NH. Cytokine removal during continuous hemofiltration in septic patients. *J Am Soc Nephrol* 1999;10(4):846–53.
- [4] Heering P, Morgera S, Schmitz FJ, Schmitz G, Willers R, Schultheiss HP, et al. Cytokine removal and cardiovascular hemodynamics in septic patients with continuous venovenous hemofiltration. *Intensive Care Med* 1997;23(3):288–96.
- [5] Sander A, Armbruster W, Sander B, Daul AE, Lange R, Peters J. Hemofiltration increases IL-6 clearance in early systemic inflammatory response syndrome but does not alter IL-6 and TNF  $\alpha$  plasma concentrations. *Intensive Care Med* 1997;23(8):878–84.
- [6] van Bommel EFH, Hesse CJ, Jutte NHPM, Zietse R, Bruining HA, Weimar W. Impact of continuous hemofiltration on cytokines and cytokine inhibitors in oliguric patients suffering from systemic inflammatory response syndrome. *Ren Fail* 1997;19(3):443–54.
- [7] Tetta C, Cavaillon J, Schulze M, Ronco C, Ghezzi P, Camussi G, et al. Removal of cytokines and activated complement components in an experimental model of continuous plasma filtration coupled with sorbent adsorption. *Nephrol Dial Transplant* 1998;13(6):1458–64.
- [8] Howell CA, Sandeman SR, Phillips GJ, Lloyd AW, Davies JG, Mikhailovsky SV, et al. The in vitro adsorption of cytokines by polymer-pyrolysed carbon. *Biomaterials* 2006;27(30):5286–91.
- [9] Sandeman SR, Howell CA, Mikhailovsky SV, Phillips GJ, Lloyd AW, Davies JG, et al. Inflammatory cytokine removal by an activated carbon device in a flowing system. *Biomaterials* 2008;29(11):1638–44.
- [10] Howell CA, Sandeman S, Webb LS, Phillips GJ, Mikhailovsky SV, Tennison S, et al. Cytokine and superantigen adsorption by novel, activated carbon beads. *Int J Artif Organs* 2008;31(7):656–656.
- [11] Weber V, Linsberger I, Ettenauer M, Loth F, Hoyhtya M, Falkenhagen D. Development of specific adsorbents for human tumor necrosis factor- $\alpha$ : influence of antibody immobilization on performance and biocompatibility. *Biomacromolecules* 2005;6(4):1864–70.
- [12] Sandeman SR, Howell CA, Phillips GJ, Lloyd AW, Davies JG, Mikhailovsky SV, et al. Assessing the in vitro biocompatibility of a novel carbon device for the treatment of sepsis. *Biomaterials* 2005;26(34):7124–31.
- [13] Ryoo R, Joo SH, Jun S. Synthesis of highly ordered carbon molecular sieves via template-mediated structural transformation. *J Phys Chem B* 1999;103(37):7743–6.
- [14] Xia YD, Mokaya R. Ordered mesoporous carbon hollow spheres nanocast using mesoporous silica via chemical vapor deposition. *Adv Mater* 2004;16(11):886–91.
- [15] Chmiola J, Yushin G, Dash R, Gogotsi Y. Effect of pore size and surface area of carbide derived carbons on specific capacitance. *J Power Sources* 2006;158(1):765–72.
- [16] Gogotsi Y, Nikitin A, Ye H, Zhou W, Fischer JE, Yi B, et al. Nanoporous carbide-derived carbon with tunable pore size. *Nat Mater* 2003;2(9):591–4.
- [17] Hoffman EN, Yushin G, Barsoum MW, Gogotsi Y. Synthesis of carbide-derived carbon by chlorination of Ti<sub>2</sub>AlC. *Chem Mater* 2005;17(9):2317–22.
- [18] Hoffman EN, Yushin G, El-Raghy T, Gogotsi Y, Barsoum MW. Micro and mesoporous Mesoporous Mater 2008;112(1–3):526–32.
- [19] Yushin G, Hoffman EN, Barsoum MW, Gogotsi Y, Howell CA, Sandeman SR, et al. Mesoporous carbide-derived carbon with porosity tuned for efficient adsorption of cytokines. *Biomaterials* 2006;27(34):5755–62.
- [20] Yushin GN, Hoffman EN, Nikitin A, Ye H, Barsoum MW, Gogotsi Y. Synthesis of nanoporous carbide-derived carbon by chlorination of titanium silicon carbide. *Carbon* 2005;43(10):2075–82.
- [21] Dash RK, Yushin G, Gogotsi Y. Synthesis, structure and porosity analysis of microporous and mesoporous carbon derived from zirconium carbide. *Microporous Mesoporous Mater* 2005;86(1–3):50–7.
- [22] Marum S, Ribeiro J, Arranhado E, Lage H, Mota L, Marcelino P, et al. Cytokines and sepsis – just black smoke? *Crit Care* 2000;4(Suppl. 1):P66.
- [23] Barsoum MW, El-Raghy T. Synthesis and characterization of a remarkable ceramic: Ti<sub>3</sub>SiC<sub>2</sub>. *J Am Ceram Soc* 1996;79(7):1953–6.
- [24] Frodelius J, Sonestedt M, Björklund S, Palmquist J-P, Stiller K, Högberg H, et al. Ti<sub>2</sub>AlC coatings deposited by high velocity oxy-fuel spraying. *Surf Coat Technol* 2008;202(24):5976–81.
- [25] Barsoum M, El-Raghy T, Ali M. Processing and characterization of Ti<sub>2</sub>AlC, Ti<sub>2</sub>AlN, and Ti<sub>2</sub>AlC<sub>0.5</sub>N<sub>0.5</sub>. *Metall Mater Trans A* 2000;31(7):1857–65.
- [26] Urbonaite S, Hålldahl L, Svensson G. Raman spectroscopy studies of carbide derived carbons. *Carbon* 2008;46(14):1942–7.
- [27] Ni ZH, Fan HM, Fan XF, Wang HM, Zheng Z, Feng YP, et al. High temperature Raman spectroscopy studies of carbon nanowalls. *J Raman Spectrosc* 2007;38(11):1449–53.
- [28] Reed C, Fu Z, Wu J, Xue Y, Harrison R, Chen M, et al. Crystal structure of TNF- $\alpha$  mutant R31D with greater affinity for receptor R1 compared with R2. *Protein Eng* 1997;10(10):1101–7.
- [29] Blick M, Sherwin SA, Rosenblum M, Gutterman J. Phase I study of recombinant tumor necrosis factor in cancer patients. *Cancer Res* 1987;47(11):2986–9.
- [30] Somers W, Stahl M, Seehra JS. 1.9 Å crystal structure of interleukin 6: implications for a novel mode of receptor dimerization and signaling. *EMBO J* 1997;16(5):989–97.
- [31] Eck MJ, Sprang SR. The structure of tumor necrosis factor- $\alpha$  at 2.6 Å resolution. Implications for receptor binding. *J Biol Chem* 1989;264(29):17595–605.
- [32] Xu G-Y, Yu H-A, Hong J, Stahl M, McDonagh T, Kay LE, et al. Solution structure of recombinant human interleukin-6. *J Mol Biol* 1997;268(2):468–81.